

Analysis of Piezoelectric Materials for Energy Harvesting Devices under High-*g* Vibrations

To cite this article: Dongna Shen *et al* 2007 *Jpn. J. Appl. Phys.* **46** 6755

View the [article online](#) for updates and enhancements.

Related content

- [Vibration energy harvesting with AlN-based piezoelectric devices](#)
R Elfrink, T M Kamel, M Goedbloed *et al.*
- [Vacuum-packaged piezoelectric vibration energy harvesters](#)
R Elfrink, M Renaud, T M Kamel *et al.*
- [Vibration Control of Piezoelectric Lead Zirconate Titanate Ceramics Using Negative Capacitance](#)
Jun Takarada, Kenji Imoto, Ken Yamamoto *et al.*

Recent citations

- [Piezoelectric energy harvester operated by noncontact mechanical frequency up-conversion using shell cantilever structure](#)
Munseon Jang *et al*
- [A Belleville-spring-based electromagnetic energy harvester](#)
Davide Castagnetti
- [A wideband fractal-inspired piezoelectric energy converter: design, simulation and experimental characterization](#)
Davide Castagnetti

Analysis of Piezoelectric Materials for Energy Harvesting Devices under High-g Vibrations

Dongna SHEN, Song-Yul CHOE¹, and Dong-Joo KIM*

Materials Research and Education Center, Auburn University, Auburn, AL 36849, U.S.A.

¹Department of Mechanical Engineering, Auburn University, Auburn, AL 36849, U.S.A.

(Received May 26, 2007; accepted July 27, 2007; published online October 9, 2007)

We analyzed the miniaturized energy harvesting devices (each volume within 0.3 cm^3) fabricated by using three types of piezoelectric materials such as lead zirconium titanate (PZT) ceramic, macro fiber composite (MFC) and poly(vinylidene fluoride) (PVDF) polymer to investigate the capability of converting mechanical vibration into electricity under larger vibration amplitudes or accelerations conditions ($\geq 1g$, gravitational acceleration). All prototypes based on a bimorph cantilever structure with a proof mass were aimed to operate at a vibration frequency of 100 Hz. PZT-based device was optimized and fabricated by considering the resonant frequency, the output power density, and the maximum operating acceleration or safety factor. PVDF- and MFC-prototypes were designed to have same resonant frequency as well as same volume of the piezoelectric materials as the PZT prototype. All three devices were measured to determine if they could generate enough power density to provide electric energy to power a wireless sensor or a microelectromechanical systems (MEMS) device without device failure. [DOI: 10.1143/JJAP.46.6755]

KEYWORDS: energy harvesting, piezoelectric material, cantilever, vibration

1. Introduction

There has been much interest in the concept of energy harvesting, which is a process of capturing the ambient waste energy and converting it into electricity. Increasing demands upon the real mobile devices such as wireless sensor networks and the recent advent of the extremely low power electrical and mechanical devices such as microelectromechanical systems (MEMS) make such energy harvesting devices attractive. A variety of ambient sources such as wind, light, thermal, and mechanical vibration have been studied as an additional energy supplier. Among them, the mechanical vibration has been considered as a potential energy source where there is insufficient light or thermal energy. Vibration source is generally ubiquitous and can be readily found in accessible locations such as air ducts and building structures. Three types of electromechanical transducers including electromagnetic, electrostatic, and piezoelectric have been utilized to design and build vibration-based energy harvesting devices. El-hami *et al.* utilized an electromagnetic transducer to realize a vibration-based electromechanical power generator.¹⁾ Miyazaki *et al.* capitalized on a variable-resonating capacitor to convert the vibration energy to electricity.²⁾ Piezoelectric energy harvesting devices have been more intensively studied because of their simple configuration, high converting efficiency, and precise control.^{3–7)} In order to achieve higher vibration-to-electricity conversion, the cantilever structure with a proof mass was mainly focused since this structure can generate a larger strain and can be easily designed to oscillate at low frequencies whose ranges are typically between 60 and 200 Hz.⁶⁾ Although many sensor devices may be located under common environmental vibrations such as a building showing moderate values of vibration amplitude ($<9.8\text{ m/s}^2$; $1g$, gravitational acceleration), they can be installed at the conditions of higher vibration amplitudes such as vehicles. Therefore, such devices will require both higher conversion efficiency and the vibration durability.

In this study, three types of piezoelectric materials such as

lead zirconium titanate (PZT) ceramic, poly(vinylidene fluoride) (PVDF) polymer, and macro fiber composite (MFC) were investigated and analyzed to determine the capability of harvesting energy under higher vibration amplitudes ($\geq 1g$) without device failure. Dimensions of the PZT prototype were designed and fabricated by considering the resonant frequency, the output power density, and the maximum operating acceleration or safety factor. The PVDF and MFC prototypes were designed by using the same volume of piezoelectric materials as the PZT prototype. Characterization such as voltage–current measurement was performed to analyze the effect of piezoelectric materials on the performance and practicability of energy harvesting devices with the consideration of power conversion circuit.

2. Experimental Procedure

2.1 Prototype fabrication

PZT, PVDF, and MFC were chosen as piezoelectric materials for energy harvesting devices from Piezo Systems (T-215-H4-103Y), Measurement Specialties (LDT0-028K/L), and Smart Material (M8507 P2). Their characteristics are summarized in Table I for comparison. From the values in Table I, PZT has the highest converting efficiency (coupling coefficient $k_{31} = 0.44$), the highest application temperature (230°C), but the lowest mechanical yield strength ($\sim 20\text{ MPa}$); PVDF shows the highest flexibility (Young's modulus = $2\text{--}4$), but the lowest converting efficiency ($k_{31} = 0.12$) and the application temperature (80°C); MFC

Table I. Characteristic comparison among three types of piezoelectric materials.

	PZT	PVDF	MFC
Maximum temperature ($^\circ\text{C}$)	230	80	180
Young's modulus (GPa)	62	2–4	16
Yield strength (MPa)	20	30	>30
d_{31} ($\times 10^{-12}\text{ m/V}$)	320	23	170
k_{31}	0.44	0.12	—
Dielectric constant	3800	12–13	—

*E-mail address: dkim@eng.auburn.edu

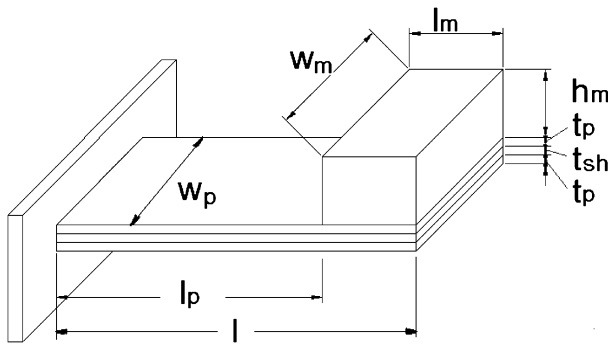


Fig. 1. The schematic diagram of cantilever configuration and parameters.

Table II. Finally designed dimensions of three types of materials.

Dimensions	PZT	PVDF	MFC
Bender length \times width \times height (mm ³)	25.00 \times 3.20 \times 0.38	10.94 \times 22.00 \times 0.354	15.80 \times 7.00 \times 0.50
Weight of proof mass (g)	0.501	3.512	2.740
Total prototype volume (cm ³)	0.0564	0.267	0.197

has the medium application temperature (180 °C) and the converting efficiency.

To analyze and evaluate the performance of energy harvesting devices depending on types of piezoelectric materials, three criteria were applied: first, the same bimorph configuration with a 0.1 mm of flexible brass center shim (as shown in Fig. 1); second, the same volume of the piezoelectric materials (~ 0.02 cm³); third, the same resonant frequencies (~ 100 Hz). The dimensions of the piezoelectric benders and the final designs are listed in Table II. Figure 2 shows the picture of the fabricated prototypes.

2.2 Experimental setup

The resonant frequency of a prototype was measured using an impedance analyzer (Agilent 4294A), and then the output signal was evaluated using the experimental setup as shown in Fig. 3. The prototype was mounted on an electromagnetic shaker (Labworks ET-132-203). The ambient vibration frequency, that is, the shaker's vibration was controlled by an external function generator (Agilent 33220A) through an amplifier connected to the shaker. The shaker was actuated by a sine wave produced from a function generator, and the vibration amplitude was controlled by the amplifier. The vibration generated from the shaker was simultaneously monitored by an accelerometer (PCB Piezoelectronics 352C65) through recording output signals of an oscilloscope (Tektronix TDS3014B). The piezoelectric prototype was connected with a series of resistors and the voltage across the resistor was measured to characterize the behaviors of generated power. The output sine wave voltage was also recorded through the digital oscilloscope and was used to calculate the output power.

3. Results and Discussion

3.1 Resonant frequency

The resonant frequency of a prototype should be designed to match the environmental vibration frequency to achieve the maximum output power. It was reported that orders of reduction in output power occur even for a small deviation of vibration frequency from the resonant frequency.⁸⁾

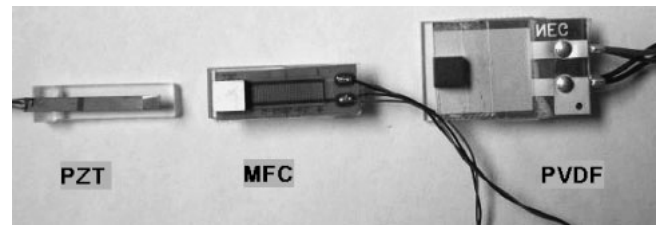
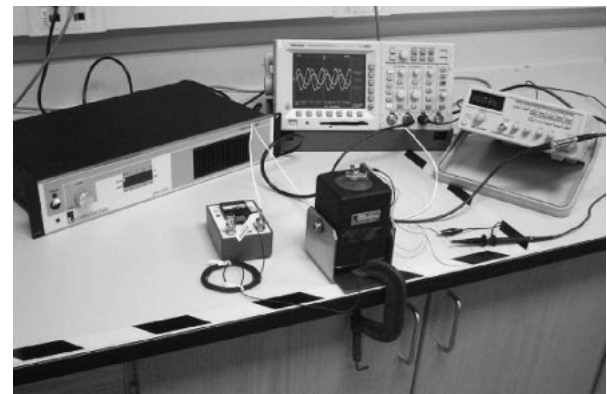
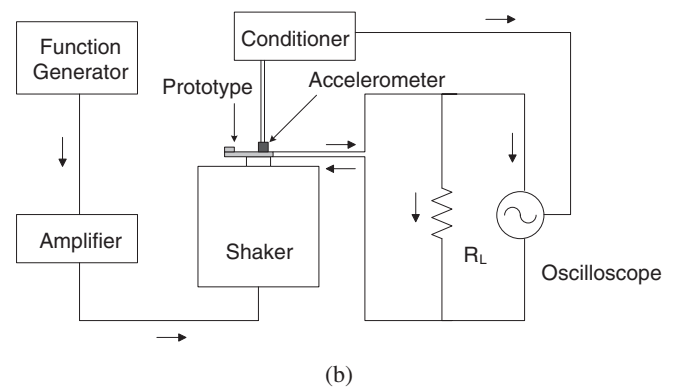


Fig. 2. The picture of fabricated prototypes using three types of piezoelectric materials.



(a)



(b)

Fig. 3. (a) The experimental setup and (b) a schematic diagram of analyzing generated power through simple resistance load under variable vibration conditions.

The resonant frequency of a bimorph cantilever beam was calculated by eqs. (1)–(4):⁹⁾

$$f_n = \frac{v_n^2}{2\pi} \sqrt{\frac{0.236w_p E_0 (l - l_m/2)^3}{0.236mw_p l^7 + \Delta m l^3 (l - l_m/2)^3}}, \quad (1)$$

$$E_0 = \frac{2E_p t_p^3}{3} + E_p t_{sh} t_p^2 + \frac{E_p t_{sh}^2 t_p}{2} + \frac{t_{sh}^3 E_{sh}}{12}, \quad (2)$$

$$m = 2\rho_p t_p + \rho_{sh} t_{sh}, \quad (3)$$

$$\Delta m = \rho_m l_m w_m h_m, \quad (4)$$

where l is the total length of the cantilever, l_m the length of the proof mass, refer to Fig. 1, m the effective mass of the bimorph bender structure only without including the proof mass, w_p the width of the bender, ρ_p , ρ_{sh} , t_p , t_{sh} , E_p , and E_{sh} respectively the densities, the thicknesses, and the Young's modulus of the piezoelectric material and the center shim metal (brass in this study), v_n a constant, n the n th mode vibration (only the first mode was considered here and $v_1 = 1.375$), Δm the proof mass, ρ_m , w_m , and h_m , respectively, the density, the width, and the height of the proof mass.

Since the prototype fabrication was performed based upon the commercially available PZT bimorphs, the thicknesses of the PZT layer and the center shim brass, and the width of the bender was predetermined from the specifications. The aimed resonant frequency, 100 Hz, was attained by varying the length of the PZT bender and the dimension of the proof mass. Tungsten was chosen as a proof mass material due to its high density. For comparative analysis of MFC- and PVDF-based prototypes, the dimensions were chosen to have same volume of piezoelectric materials as the PZT-based prototype.

The resonant behaviors of three prototypes were measured as shown in Fig. 4. The resonant frequencies of PZT, PVDF, and MFC-devices were about 97.6, 103.7, and 98.5 Hz, respectively. The difference between the calculation and the measurement was within 5% error. For the PZT-based prototype, the phase angle changed sharply at the resonant frequency, while the changes observed in the PVDF- and MFC-prototypes were not sharp and showed more noisy signals, especially for the PVDF prototype. These can result from different dielectric properties of three piezoelectric materials such that lower charges generated from PVDF and MFC may lead to lower signal to noise ratio. In addition, different bending behaviors due to the rigidity of materials and the fixture conditions may be also reasons for such noise. These are believed to be factors influencing the output voltage or power by changing the damping ratio, which will be discussed in later sections.

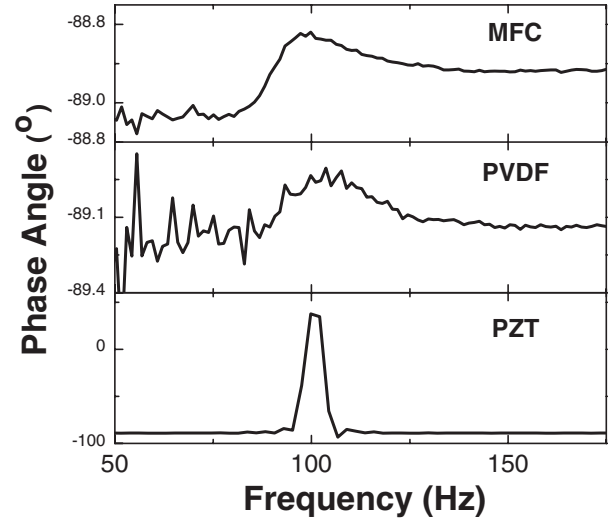


Fig. 4. The measured resonant frequencies of devices from three types of piezoelectric materials.

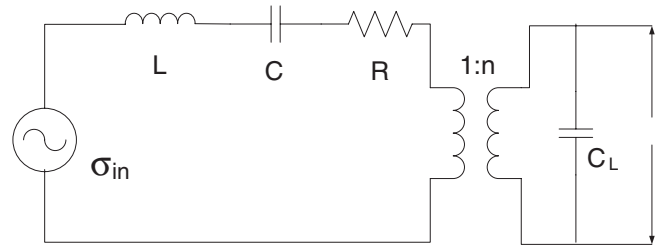


Fig. 5. The equivalent circuit model for a PZT power generator.

3.2 Output power density with a simple resistance load

The output power analysis was performed based on the reported model,^{6,9)} which is derived from an electric equivalent circuit model (as shown in Fig. 5) for a PZT beam, where a voltage source connects in series to an inductor, a resistor, and a capacitor in a resonant circuit. The formulae used for calculating output power are eqs. (5)–(9):

$$P = \frac{|V|^2}{R_{Opt}}, \quad (5)$$

$$V = \frac{-j\omega \frac{E_p d_p}{\epsilon} b^*}{\left[\frac{1}{RC} \omega_r^2 - \left(\frac{1}{RC} + 2\zeta \omega_r \right) \omega^2 \right] + j\omega \left[\omega_r^2 (1 + k^2) + \frac{2\zeta \omega_r}{RC} - \omega^2 \right]} A_{in}, \quad (6)$$

$$R_{Opt} = \frac{2\zeta}{\omega C \sqrt{4\zeta^2 + k^2}}, \quad (7)$$

$$b^* = \frac{3b}{l_p^2} \cdot \frac{2l_p + l_m - l_e}{2l_p + 1.5l_m}, \quad (8)$$

$$C_p = \frac{2\epsilon w_p l_e}{t_p}, \quad (9)$$

where P and V are the power and the potential generated in a piezoelectric cantilever, R_{Opt} the optimal resistance load where the maximum power attained, d the piezoelectric constant, ω the angular frequency of the input driving vibration, ω_r the resonant angular frequency of the cantilever with a proof mass, ζ the damping ratio of the device (0.01 for the PZT, measured), k the coupling coefficient (0.2 for the PZT, measured), l_p the length of the PZT without the proof mass, l_e the length of the electrode on each side of the PZT bender, here $l_e = l_p$, C the capacitance of the cantilever.

lever bender, ε the dielectric constant of the piezoelectric material.

The output-peak voltages were first measured with varying load resistors at given vibration acceleration and the power density was calculated after considering the volume of devices. The generated current from the devices is also calculated by Ohm's Law to provide the guide of choosing power management electronics such as rectifier and dc-dc converter. The relationships of the peak power density and the voltage versus the current density of three prototypes are shown in Fig. 6 at 1g acceleration condition. The optimal resistance loads of these three prototypes were found to be 73 k Ω (PZT), 900 k Ω (PVDF), and 55 k Ω (MFC) by measuring the output voltage with varying the resistors. There are reasons why the optimal resistance loads determined by experiment are not consistent with eq. (7) such as unavoidable parasitic damping and excessive device amplitude at higher vibration leading to nonlinear behavior, which introduces difficulties in keeping the generator operating at resonance. At the optimal resistance loads determined by measurement, the output voltages were separately recorded as shown in Fig. 7. The power densities were then calculated by considering the total volumes of prototypes. The relationships of the output peak voltage and the power density as a function of ambient vibration frequency such as 1, 3, and 5g acceleration are summarized and compared in Table III. Figure 8 shows the results measured at 1g conditions. The power densities of the MFC and the PVDF prototypes are 17 and 9 $\mu\text{W}/\text{cm}^3$ respectively, while the power density obtained from the PZT prototype is 9,184 $\mu\text{W}/\text{cm}^3$, which is approximately 540 and 1000 times larger than the output of the MFC and the PVDF prototypes. With increasing acceleration, the generated voltage increases exponentially. Therefore, higher vibration condition will allow the miniaturized devices from MFC and PVDF to achieve the minimum power density required to supply power to a microscale device based on reported values, that is, above 300 $\mu\text{W}/\text{cm}^3$.^{3,7)} These output data indicate that PZT could be the best candidate as a piezoelectric material for vibration energy harvesting in comparison with MFC and PVDF. Another factor for consideration is current through the piezoelectric devices. In general, the power in these devices is mainly due to higher voltage than current. Electronic components used in the energy harvesting devices such as DC voltage regulators or microsensors, however, operate with minimal current on the order of a few microamperes. As seen in Fig. 6, the current generated at 1g condition and with about 0.02 cm^3 volume of piezoelectric materials were about 81, 1.8, and 8.1 μA for PZT-, PVDF-, and MFC-based devices, respectively. Low current values in PVDF and MFC-based devices can have the limit of scaling to realize miniaturization.

Another observation from Fig. 8 is that the maximum values of the power or the power density were obtained when the ambient vibration frequency was matching with the measured resonant frequency of a prototype at 1g acceleration. Interestingly, when a prototype is under a high-g vibration conditions, the peak frequency where maximum output attained apparently shifts to the lower value. For the PVDF prototype, the shift of the peak frequency is 5.1 Hz. The shifts for the PZT- and the MFC-

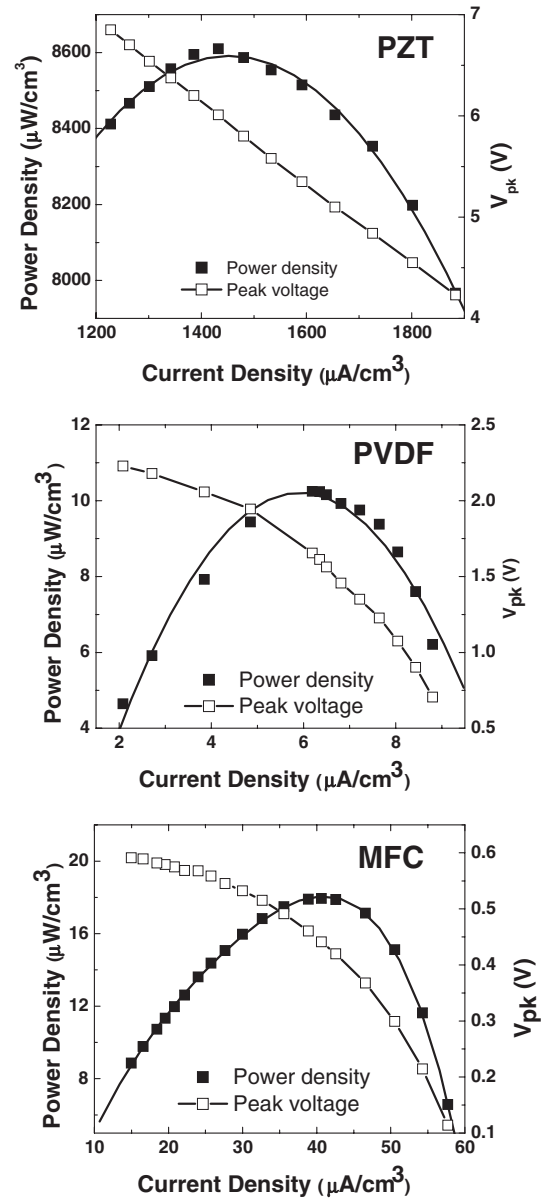


Fig. 6. Power density and voltage as a function of current density obtained using various external resistors.

based prototypes are 11.0 and 7.5 Hz, respectively. It has been observed that the peak frequency shift decreases at a low-g vibration condition, that is, the lower input magnitude of the vibration is applied to the same prototype. This phenomenon could be due to the combined effects from the increasing effective mass and the elastic nonlinearity with higher cantilever beam deflections that occur at higher vibration conditions.

3.3 Safety factor comparison

The potential fracture or damage of the piezoelectric materials under high-vibration conditions can limit the applications requiring severe vibrations such as vehicle conditions. To evaluate the robustness of a cantilever structure, the safety factor (S) was introduced and calculated by eqs. (10)–(14):

$$S = \frac{\sigma_{ys}}{\sigma_{\max}}, \quad (10)$$

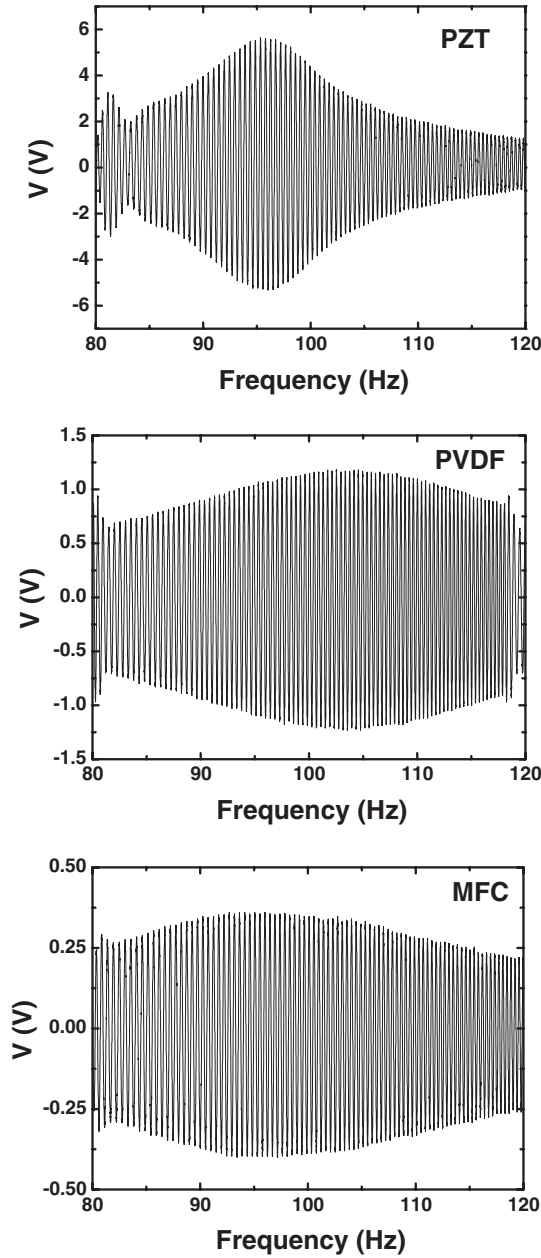


Fig. 7. Output voltage waveforms of three piezoelectric devices as a function of vibration frequency.

$$\sigma_{\max} = \frac{M(t_{\text{sh}}/2 + t_p)}{I}, \quad (11)$$

$$I = 2 \left(\frac{w_p t_p^3}{12} + w_p t_p b^2 \right) + \frac{1}{12} \frac{E_{\text{sh}}}{E_t} w_p t_{\text{sh}}^3, \quad (12)$$

$$b = \frac{t_p + t_{\text{sh}}}{2}, \quad (13)$$

$$M = \Delta m g \left(l_p + \frac{l_m}{2} \right) + m g \frac{(l_p + l_m)^2}{2} w_p, \quad (14)$$

where σ_{ys} is the yield strength of the weakest material, σ_{\max} the maximum stress generated in the bender surface at the clamping area, M the moment of the cantilever with a proof mass, I the moment of inertia of the cantilever, here the proof mass was simplified into a point at the middle of the proof mass, other parameters are the same as before.

The output power densities of the PVDF and MFC devices

Table III. Characteristic comparison of three prototypes.

Characteristics	PZT	PVDF	MFC
Resonant frequency (Hz)	97.6	103.7	98.5
Optimal resistance (k Ω)	73	900	55
Current density with R_{Opt} at 3g ($\mu\text{A}/\text{cm}^2$)	2,722	6.2	40.7
Power density at different acceleration ($\mu\text{W}/\text{cm}^2$)			
1g	8,600	9	17
3g	62,300	67	150
5g	150,100	188	387
Safety factor at different acceleration			
1g	12.0	266	113
3g	4.0	89	38
5g	2.4	53	23

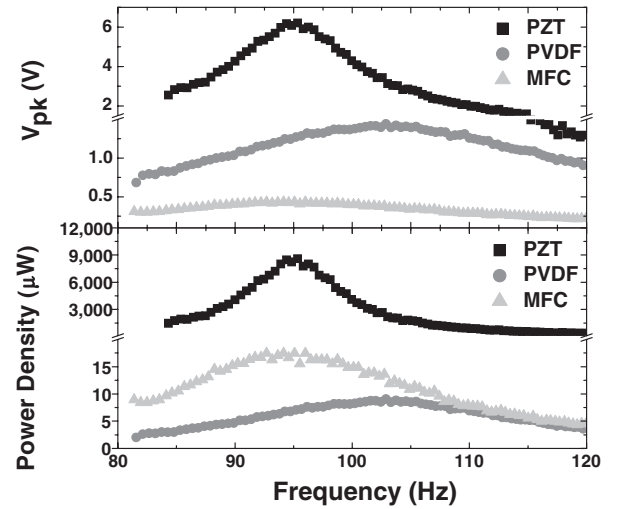


Fig. 8. The output peak power and voltage as a function of environmental vibration frequency.

were measured to be much lower than that of the PZT device. Under severe vibration conditions, however, PVDF and MFC are more robust compared with PZT due to less fragility of piezoelectric materials. Table III shows the comparison of the safety factors calculated at 1, 3, and 5g among three prototypes. The PVDF prototype shows the highest fracture strength, and the fracture strength of the MFC prototype is twice lower than that of the PVDF prototype, but the fracture strength of the PZT prototype is about one order of magnitude lower than that of the PVDF prototype, that is, 12 vs 266. These results mean that it is likely safe when operating the PVDF and the MFC prototypes above 100g, but the damage of the PZT prototype is highly probable when operating over 10g. When considering structural robustness, therefore, PVDF and MFC show the potentials at harsh vibration environments, while PZT should be designed to withstand higher vibration conditions by considering smaller proof mass, limiting maximum strain, etc.

4. Conclusions

Cantilever power harvesting prototypes made of three types of piezoelectric materials such as PZT ceramic, MFC, and PVDF polymer were designed and fabricated. Devices with the same volume of piezoelectric materials were evaluated by varying the load resistance, the ambient

vibration frequency and amplitude, and the maximum fracture strength of each prototype was estimated from the proposed equations and verified. PZT-based device shows the highest power and current densities among three devices. The damage of a piezoelectric material determined by calculating fracture strength, however, can limit its applications into low-g vibration conditions unless further modification of design. For such harsh vibration conditions, MFC and PVDF show the potentials. However, the current generation in these devices is limited by the size of piezoelectric materials.

Acknowledgment

Authors would like to thank Auburn University Detection and Food Safety Center (AUDFS) and industry for financial support.

- 1) M. El-hami, P. Glynn-Jones, N. M. White, M. Hill, S. Beeby, E. James, A. D. Brown, and J. N. Ross: *Sens. Actuators A* **92** (2001) 335.
- 2) M. Miyazaki, H. Tanaka, G. Ono, T. Nagano, N. Ohkubo, T. Kawahara, and K. Yano: *Proc. Int. Symp. Low Power Electronics and Designs*, 2003, p. 193.
- 3) H. W. Kim, A. Batra, S. Priya, K. Uchino, D. Markley, R. E. Newnham, and H. F. Hofmann: *Jpn. J. Appl. Phys.* **43** (2004) 6178.
- 4) T. Endow and S. Hirose: *Jpn. J. Appl. Phys.* **42** (2003) 6128.
- 5) J. Ajitsaria, S. Y. Choe, D. Shen, and D. J. Kim: *Smart Mater. Struct.* **16** (2007) 447.
- 6) S. Roundy, P. K. Wright, and J. Rabaey: *Comput. Commun.* **26** (2003) 1131.
- 7) M. J. Ramsay and W. W. Clark: *Proc. SPIE* **4332** (2001) 429.
- 8) S. Roundy, E. S. Leland, J. Baker, E. Carleton, E. Reilly, E. Lai, B. Otis, J. M. Rabaey, P. K. Wright, and V. Sundararajan: *IEEE Pervasive Comput.* **4** (2005) No. 1, 28.
- 9) D. Shen, J. Ajitsaria, S. Y. Choe, and D. J. Kim: *Mater. Res. Soc. Symp. Proc.* **888** (2006) 271.